Eur Biophys J (2008) 37:701–709
DOI 10.1007/s00249-008-0324-x

ORIGINAL PAPER

The role of protein–solvent hydrogen bond dynamics in the structural relaxation of a protein in glycerol versus water

Mounir Tarek · Douglas J. Tobias

Received: 12 October 2007 / Revised: 28 March 2008 / Accepted: 1 April 2008 / Published online: 22 April 2008

Abstract We used MD simulations to investigate the dependence of the dynamics of a soluble protein, RNase A, on temperature and solvent environment. Consistent with neutron scattering data, the simulations predict that the protein undergoes a dynamical transition in both glycerol and aqueous solutions that is absent in the dry protein. The temperature of the transition is higher, while the rate of increase with temperature of the amplitudes of motion on the 100 ps timescale is lower, in glycerol versus water. Analysis of the dynamics of hydrogen bonds revealed that the protein dynamical transition is connected to the relaxation of the protein–solvent hydrogen bond network, which, in turn, is associated with solvent translational diffusion. Thus, it appears that the role of solvent dynamics in affecting the protein dynamical transition is qualitatively similar in water and glycerol.

Keywords Molecular dynamics · Protein dynamics · Dynamical transition · Protein hydration · Hydrogen bonds

Advanced neutron scattering and complementary techniques to study biological systems. Contributions from the meetings, "Neutrons in Biology", STFC Rutherford Appleton Laboratory, Didcot, UK, 11–13 July and "Proteins At Work 2007", Perugia, Italy, 28–30 May 2007.

M. Tarek
Equipe de dynamique des assemblages membranaires,
Unité mixte de recherche CNRS/UHP 7565,
Université Henri Poincaré, BP 239,
54506 Vandoeuvre-lès-Nancy cedex, France

D. J. Tobias (✉)
Department of Chemistry, University of California,
Irvine, CA 92697-2025, USA
e-mail: dtobias@uci.edu

Introduction

Under physiological conditions in their native environments, proteins visit a vast number of conformations, commonly referred to as substates, in the vicinity of a well-defined three-dimensional structure (Frauenfelder et al. 1991). The energy landscapes of proteins appear to be organized into a hierarchy of levels, with the top level containing only a few substates that interconvert slowly via large-scale conformational changes, and the lowest level containing a very large number of substates that interconvert by motions on the ps-ns timescales (Fenimore et al. 2004a, b). Transitions between the top level substates are rare events that are often directly associated with protein function, e.g., enzyme catalysis (Dioumaev and Lanyi 2007), while transitions between the lowest level substates are generally considered to provide the lubrication that promotes larger-scale conformational changes (Fenimore et al. 2004a, b). The precise connection between biological function and fast protein conformational fluctuations is a subject of current research and debate (Daniel et al. 2003; Doster and Settles 2005; Heberle et al. 2000; Kurkal et al. 2005; Lechner et al. 2006).

The influence of the environment on the dynamics of the lowest level protein substates is the main subject of this paper. In addition to contributing to additional insight into the connection between protein dynamics and function, a fundamental understanding of the coupling between protein and solvent dynamics is already advancing the science of bioprotection, e.g., of biomolecule-based pharmaceuticals (Caliskan et al. 2004; Curtis et al. 2006), which is of potential practical value in the food and pharmaceutical industries, and could also prove useful in the optimization of the design of biomimetic materials (e.g., artificial photosynthetic devices and biosensors).

The so-called dynamical transition has served for almost two decades as a paradigm for investigating the coupling of the dynamics of a protein molecule and its environment. The dynamical transition is a sudden increase in the amplitudes of atomic fluctuations as a protein is heated from low temperature, and it is regarded to reflect a change in motion from solid-like (harmonic) to liquid-like (anharmonic, diffusive) (Doster et al. 1989, 1990). The transition has been detected using several experimental techniques (Doster et al. 1989; Frauenfelder et al. 1979; Knapp et al. 1982; Lee and Wand 2001; Parak 2003; Rasmussen et al. 1992; Smith et al. 1990; Tarek et al. 2000), but is most often studied using incoherent neutron scattering measurements, which probe single-particle dynamics on timescales of ps-ns and length scales of Å-nm, and make use of H/D contrast to isolate the motion of specific components in the system (Beé 1988). The solvent dependence of the dynamical transition is a clear indication of the dramatic effect of the environment on the dynamics of soluble proteins: the transition is absent in dehydrated proteins, and the extent of motion above the transition temperature, as well as the transition temperature itself, depend on solvent viscosity (Caliskan et al. 2002; Cornicchi et al. 2006; Doster and Settles 1999, 2005; Finkelstein et al. 2007; Paciaroni et al. 2002; Tsai et al. 2000). The concept of "slaving" has been invoked to discuss the control of protein motion by solvent motion (Fenimore et al. 2002; Frauenfelder et al. 2002). Recent experimental and theoretical investigations have discussed the connection of the protein dynamical transition to solvent dynamics in terms of concepts from glass physics (Chen et al. 2006; Kumar et al. 2006; Swenson et al. 2006; Zanotti et al. 2005).

The microscopic details of the coupling between protein and solvent dynamics have begun to emerge from both experimental and theoretical investigations. The observation that diffusive motion in proteins is suppressed by dehydration suggests that water molecules participate in some sort of bond-breaking process that is coupled to the protein structural relaxation (Doster and Settles 1999). The surface of a dehydrated protein is rigidified by strong (electrostatic and H-bonding) interactions between polar side chains. Protein–water H-bonds break up these interactions, and water mobility is expected to facilitate protein conformational fluctuations. Time-resolved mean-squared displacements of protein hydration water derived from neutron scattering of a soluble protein have revealed the onset of water translational diffusion at the protein dynamical transition (Doster and Settles 2005). Recent neutron scattering experiments have shown that the structural and dynamical properties of the interfacial water strongly influence the side chain dynamics and the activation of diffusive motion in model peptides (Russo et al. 2007). MD simulations by others and us have elucidated the microscopic mechanism of the solvent control of fast dynamics in soluble proteins. In the case of hydrated soluble proteins, we suggested that the dynamical transition requires relaxation of the protein–water hydrogen bond network, which, in turn, requires the onset of water translational diffusion (Tarek and Tobias 2002). A similar conclusion was subsequently reached by others (Tournier et al. 2003), and an analogous mechanism has been proposed to apply in the case of glycerol solvation (Dirama et al. 2005). Our theoretical predictions concerning the coupling of protein and water dynamics were recently confirmed by a recent investigation, combining neutron scattering with selective deuteration and MD simulations of the solvent-coupled dynamical transition of a soluble protein in a hydrated powder sample (Wood et al. 2008).

In this paper, we report an MD simulation study of the dynamical transition of a soluble protein, RNase A, in the glass-forming solvent glycerol. Our primary objective is to determine whether or not the concept that we proposed previously based on MD simulations of RNase A in water, namely, that the protein transition is triggered by relaxation of the protein–water hydrogen bond network, which, in turn, accompanies the onset of water translational diffusion, can be extended to glycerol. To this end, we directly compare results obtained from simulations of the same protein in both water and glycerol, and we find that, indeed, the mechanism of solvent activation of the dynamical transition is essentially the same in the two solvents. In addition, we further demonstrate the utility of using MD simulations to study the solvent dependence of the protein dynamical transition by showing that the transition is absent in simulations of a dry protein, consistent with experimental measurements.

Materials and methods

Set-up of the dry and hydrated protein systems

The simulations of RNase were all initiated from a crystal structure (PDB entry 7RSA) (Wlodawer et al. 1988). The simulations of the dry and hydrated protein have been described at length elsewhere (Tarek et al. 2000; Tarek and Tobias 1999, 2000). We therefore only briefly summarize here the set-up procedure and run parameters. The dry powder model contains eight protein molecules replicated by periodic boundary conditions, constructed from four unit cells (a $2a \times 2b \times c$ lattice) of the monoclinic crystal with the water molecules removed. A constant volume MD simulation at 500 K was run to produce non-native, disordered configurations on the surfaces of the protein molecules. A constant pressure run at 300 K, during which

the system contracted, enabling the protein molecules to interact with their neighbors and periodic images, followed. The system was then hydrated to $h = 0.05$ (g D_2O per g protein), corresponding to "dry" samples employed in scattering experiments, by adding 280 water molecules. The hydrated powder model was constructed from a single unit cell of the RNase A crystal. Our previous studies indicated no significant change in the protein and solvent dynamics between the powder simulations at high hydration and the crystal simulations (Tarek et al. 2000; Tarek and Tobias 1999). To construct the hydrated powder model, the monoclinic unit cell containing two protein molecules was generated from the asymmetric unit (one molecule), by using the symmetry operations of the $P21$ space group. The empty space in the cell was filled with water molecules, and the positions of the waters were relaxed by energy minimization and MD with periodic boundary conditions until the pressure stabilized in the field of the protein molecules, whose positions were held fixed. Interactions of the water molecules with each other and the proteins opened new vacancies for additional water molecules. The procedure of adding water molecules was repeated until there was no more empty space in the unit cell (six addition/annealing cycles). The final hydrated powder model consisted of two RNase A molecules and 817 water molecules, corresponding to $h = 0.57$.

Set-up of the protein in glycerol

A single RNase A molecule was placed in the center of a previously equilibrated box of glycerol molecules, and all glycerol molecules in contact with the protein were removed. We chose to consider a protein in excess glycerol (90% by weight) in order to clearly identify the influence of the solvent. This resulted in a system containing one RNase A and 1,467 glycerol molecules in a cubic box, roughly 60 Å to a side. After minimization of the energy, short constant volume and constant temperature runs were used to relax the initial system. All subsequent runs were performed at constant temperature and a constant pressure of 1 atm.

Details of the simulations

The CHARMM22 and TIP3P force fields (MacKerell Jr. et al. 1998) were used for the protein and water molecules, respectively. The force field for glycerol was compiled by choosing the appropriate parameters from the alcohol moieties in the CHARMM22 protein force field. The MD simulations were performed using the PINY_MD program (Tuckerman et al. 2000). Three-dimensional periodic boundary conditions were applied and the Ewald sum was used to calculate the electrostatic energies, forces, and virial in all of the simulations. The Lennard–Jones interactions and the real-space part of the Ewald sum were smoothly truncated at 10 Å, and long-range corrections to account for the neglected interactions were included in the energies and pressures (Allen and Tildesley 1989). The reciprocal space part of the Ewald sum was calculated using the smooth particle mesh method (Essmann et al. 1995). The Nosé–Hoover chain method (Martyna et al. 1992) was used to control the temperature in all of the simulations, with separate thermostat chains for the water, or glycerol and protein molecules. The constant pressure simulations were carried out in a fully flexible simulation box by using the extended system algorithm of Martyna et al. (1994). A multiple time step algorithm (Martyna et al. 1996) was used to integrate the equations of motion with a 4 fs time step. The lengths of bonds involving H/D atoms were held fixed by using the *shake/rattle/roll* algorithm (Andersen 1983; Martyna et al. 1996; Ryckaert et al. 1977).

Data analysis

The amplitudes of protein motion have been quantified in terms of atomic mean square fluctuations:

$$\left\langle \Delta r_j^2 \right\rangle = \left\langle \left(\mathbf{r}_j - \left\langle \mathbf{r}_j \right\rangle \right)^2 \right\rangle \tag{1}$$

where $\mathbf{r}_j$ is the position vector of atom j, and the angular brackets denote an average over time (and in some cases, atoms). To depict time dependence, we report the self-intermediate scattering functions, $I_{\mathrm{inc}}(\mathbf{Q},t)$:

$$I_{\mathrm{inc}}(\mathbf{Q},t) = \left\langle e^{i\mathbf{Q}\cdot\mathbf{r}_j(t)} e^{-i\mathbf{Q}\cdot\mathbf{r}_j(0)} \right\rangle. \tag{2}$$

Here, the angular brackets denote an average over time origins and scatterers, and $\mathbf{Q}$ is the wave vector transfer. In the calculation of the intermediate scattering function we only include the non-exchangeable protein hydrogen atoms because they dominate the spectra measured by incoherent neutron scattering experiments. The results reported in this paper are "powder averages" of $I_{\mathrm{inc}}(\mathbf{Q},t)$ computed at eight randomly chosen scattering vectors with $|\mathbf{Q}| = Q$.

As in a previous study (Tarek and Tobias 2002), we analyzed the protein–water and protein–glycerol hydrogen bond using quantities that distinguish between the fast (ps) formation and breaking of hydrogen bonds due to solvent liberation-rotation, and the slower (tens of ps) relaxation of the protein–solvent hydrogen bond network due to solvent diffusion. Specifically, we define the fast hydrogen bond lifetime, τ_{HB}, as the average time that a given protein–solvent hydrogen bond remains intact. The slow hydrogen bond network relaxation time, τ_{R}, is derived from the hydrogen bond correlation function (Luzar and Chandler 1996a, b),

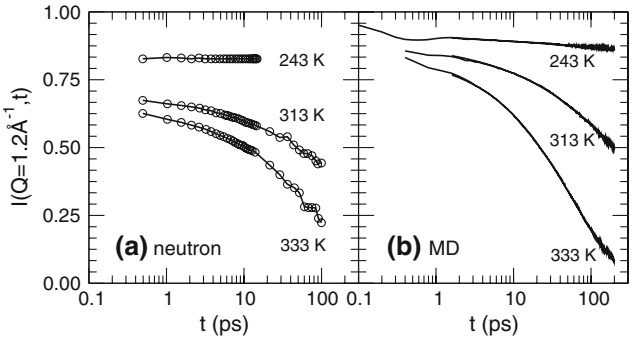

Fig. 1 Incoherent (self) intermediate scattering functions for non-exchangeable hydrogen atoms of glycerol from MD simulations at 243, 313 and 333 K

$$c(t) = \langle h(0)h(t)\rangle / \langle h(t)\rangle, \tag{3}$$

where $h(t) = 1$ if pairs are bonded at time t, and 0 otherwise. The function $c(t)$ can be viewed as probability that a random donor–acceptor pair that is initially hydrogen bonded is still bonded at time t. Hence, beyond an initial transient period, the decay of $c(t)$ is not determined by fast hydrogen bond breaking events, but rather by rearrangement of the protein–solvent hydrogen bond network. We define τ_R, the hydrogen bond network relaxation time, as the time needed for $c(t)$ to decay to $1/e$.

Results and discussion

We begin by validating the glycerol model used in the simulations. Figure 1b reports the intermediate scattering functions for glycerol non-exchangeable hydrogen atoms calculated from the MD simulations of neat glycerol at three temperatures. These results may be compared with corresponding results obtained by Wuttke et al. (1995) by Fourier inversion of incoherent neutron scattering data, reproduced in Fig. 1a. In agreement with the experiment, the scattering functions computed from the MD simulations show a fast (sub-ps) initial relaxation at all temperatures considered, and a secondary relaxation above 300 K that becomes more pronounced with increasing temperature. Although the extent of the initial (sub-ps) drop in $I(Q,t)$ is slightly less than in the experimental data,

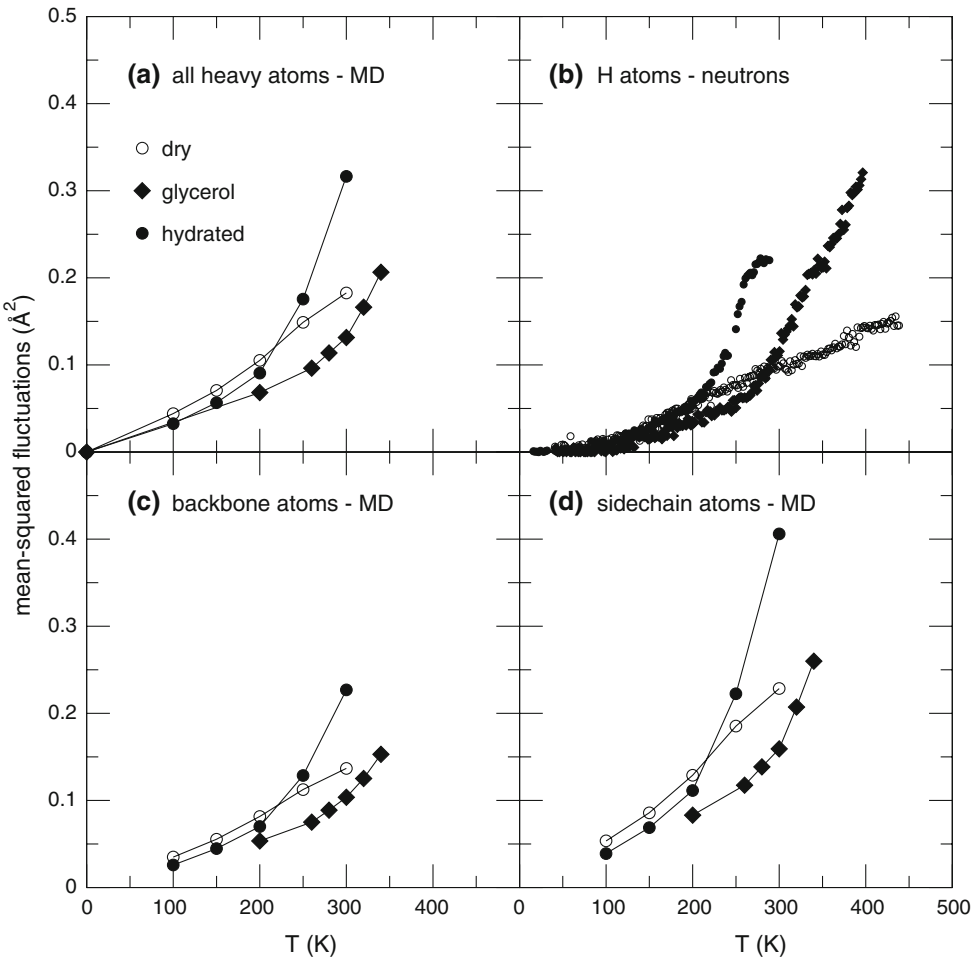

Fig. 2 Temperature dependence of atomic mean-squared fluctuations (MSFs) of RNase A in different environments: dry powder (*open circles*), hydrated powder (*filled diamonds*), glycerol (*filled circles*). **a** MSFs of all heavy atoms from MD simulation. **b** MSFs of nonexchengeable hydrogen atoms in lysozyme from elastic neutron scattering measured at an energy resolution of 1 μeV, corresponding to a timescale in the order of 100 ps (Tsai et al. 2000). **c** MSFs of backbone (C^a) atoms from MD simulation. **d** MSFs of side chain heavy atoms from MD simulations. All of the MSFs reported from the MD simulations are averages over blocks of 100 ps

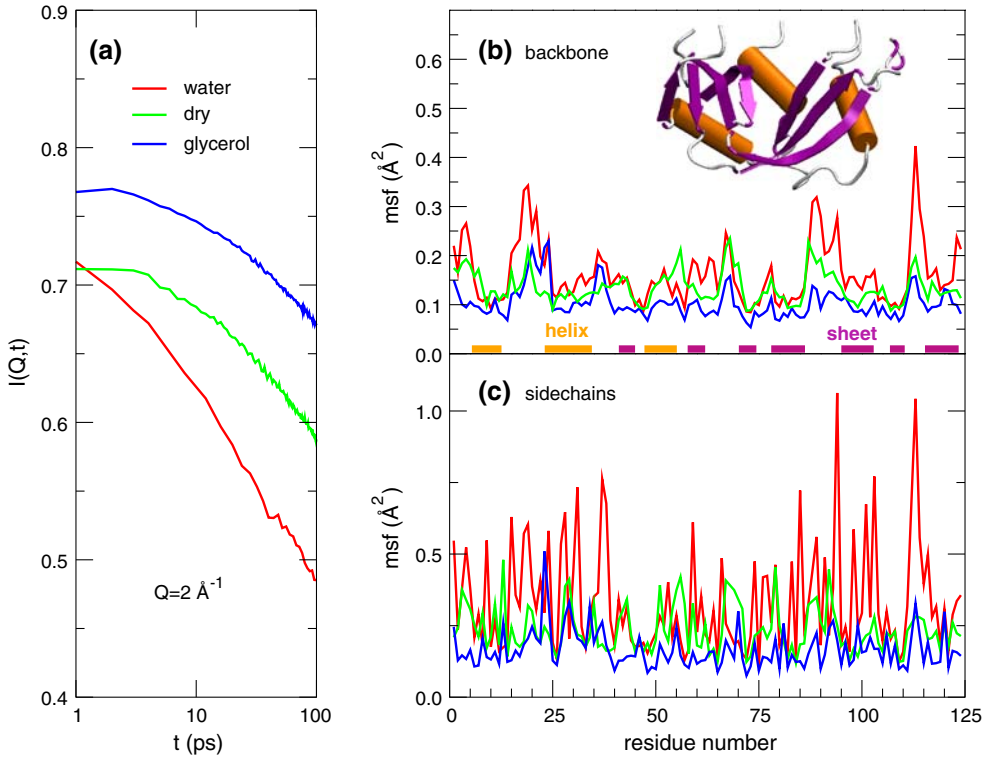

Fig. 3 Incoherent (self) intermediate scattering functions for non-exchangeable hydrogen atoms (**a**), and mean-squared fluctuations (msf) averaged over 100 ps blocks for protein backbone (**b**) and side chain (**c**) atoms of dry RNase (*green*), hydrated RNase (*red*) and RNase in glycerol (*blue*) at 300 K. The location of secondary structural elements (α helices and β sheets) in the RNase A sequence are indicated by *bars* at the bottom of (**b**), colored to correspond to the molecular graphics image of RNase A shown in the *inset*

overall the agreement between the MD and experimental results for the temperature dependence of the dynamics of neat glycerol is excellent.

The temperature dependence of the dynamics of dry RNase, and RNase in glycerol and in the hydrated crystal, is depicted in terms of the mean-squared fluctuations, averaged over all protein heavy atoms in 100 ps blocks from the MD simulations, plotted in Fig. 2a. A dynamical transition is not observed in the dry protein, as the fluctuations increase essentially linearly with temperature, while in both solvents, a dynamical transition is signaled by an abrupt increase in the fluctuations. In water (hydrated crystal), the transition occurs at about 200 K, while in glycerol it occurs at about 280 K. The simulation results are in good agreement with the mean-squared displacements for non-exchangeable H atoms in lysozyme derived by Tsai et al. (2000) from elastic neutron scattering data (Fig. 2b). Specifically, the temperatures of the transitions in both water and glycerol, the absence of a transition in the dry protein and the significant reduction of the amplitudes in the low temperature, linear (harmonic) regime in glycerol versus in the dry and hydrated protein are all well reproduced by the simulations. Figures 2c and d show the breakdown of the data into contributions from protein backbone and side chain heavy atoms, respectively, information that is not accessible to neutron experiments, which probe the motion of hydrogen atoms. The simulations indicate that the temperature and solvent dependence of the fluctuations are qualitatively similar throughout the protein, i.e., both the side chains and the backbone atoms fluctuations are suppressed going from the hydrated sample to the dry sample to the sample solvated with glycerol. As expected, the fluctuations at a given temperature in a particular solvent environment are larger for side chain versus backbone atoms.

Solvent effects on the protein dynamics at 300 K are exposed in greater detail in Fig. 3. The intermediate scattering functions displayed in Fig. 3a show two interesting features. First, the fast (sub-ps) initial decay (β relaxation) has a similar extent in both the dry and hydrated protein, while it is less pronounced in glycerol. This is consistent with the lower mean-squared fluctuations in the low temperature, harmonic regime in glycerol versus in the dry and hydrated protein (Fig. 2). Second, the secondary (α) relaxation of $I(Q,t)$ in glycerol tracks that of the dry protein, while the decay in water is significantly faster at 300 K. Figures 3b and c show the sequence dependence of the heavy atom mean-squared fluctuations in the backbone and side chains, respectively. The backbone fluctuations reflect the secondary structure of the protein, with lower

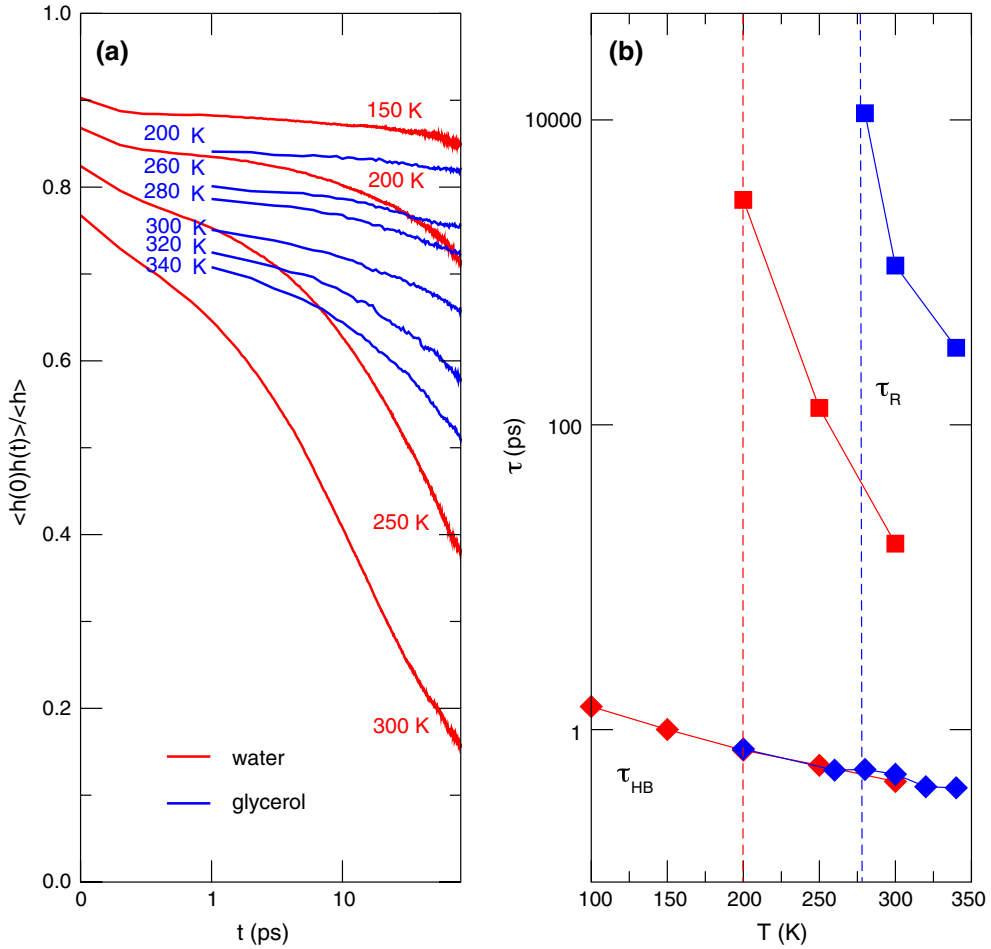

Fig. 4 **a** Time evolution of the protein–solvent hydrogen bond correlation function at several temperatures in water (*red*) and glycerol (*blue*). **b** Temperature dependence of the protein–solvent hydrogen bond lifetime, τ_{HB} (*diamonds*), and hydrogen bond network relaxation time, τ_R (*squares*), in water (*red*) and glycerol (*blue*). The *red* and *blue dashed vertical lines* indicate the temperatures of the dynamical transitions in water (~200 K) and glycerol (~280 K), respectively

fluctuations corresponding to α helices and β sheets, and higher fluctuations to connecting loops and termini. Dehydration or replacement of water by glycerol suppresses the fluctuations throughout the protein, more so in the more mobile side chains than in the backbone. Glycerol clearly has a substantially greater dynamical suppression effect at 300 K than does dehydration.

In Fig. 4, we report data that confirm our previous suggestion that the dynamical transition in soluble proteins is associated with relaxation of the protein–solvent hydrogen bond network (Tarek and Tobias 2002). The protein–solvent hydrogen bond correlation functions displayed in Fig. 4a show a fast initial decay corresponding to hydrogen bond breaking by librational motion. Above the protein dynamical transition temperature in each solvent (~200 K in water, ~280 K in glycerol), the correlation functions exhibit a secondary decay that becomes more pronounced with increasing temperature. This decay is essentially absent below the dynamical transition temperature, indicating a structural arrest of the protein–solvent hydrogen bond network. The timescales of fast and slow protein–solvent hydrogen bond dynamics are plotted as a function of temperature in Fig. 4b. The timescale of the fast hydrogen bond dynamics, τ_{HB}, is very similar in both water and glycerol, and in both cases there is only a weak dependence on temperature over a broad range spanning the protein dynamical transitions (indicated by dashed lines in Fig. 4b). On the other hand, the timescale, τ_R, of the secondary decay in the hydrogen bond correlation functions, displays a strong dependence on temperature, and appears to diverge as the temperature is lowered toward the protein dynamical transition temperature. Thus, there appears to be a strong correlation between the relaxation of the protein–solvent hydrogen bond network and the protein dynamical transition in both glycerol and water.

In a previous investigation, we showed that the relaxation of the protein–water hydrogen bond network is tied to

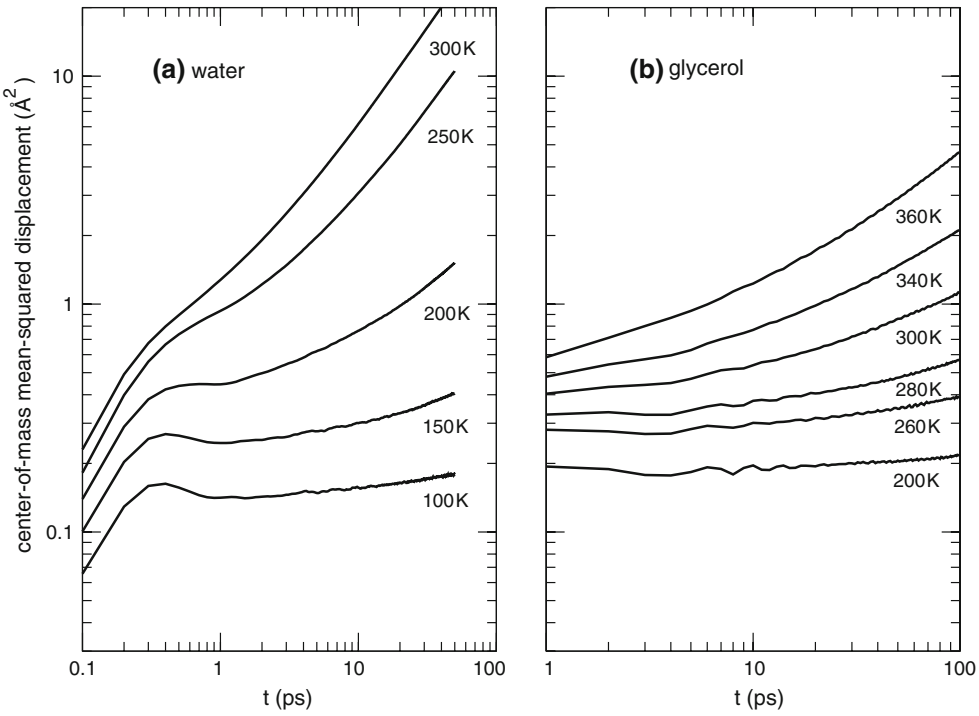

Fig. 5 Time evolution of the center of mass mean-squared displacement of the solvent in the protein–solvent systems at several temperatures: **a** water; **b** glycerol

water translational diffusion (Tarek and Tobias 2002). This is evident in Fig. 5a, where we plot the time evolution of the water center of mass mean-squared displacement over a range of temperatures spanning the protein dynamical transition. The curves all display a rapid (sub-ps) initial jump, corresponding to ballistic motion, i.e., the motion of water molecules before they hit the cage formed by their immediate neighbors. Above the protein dynamical transition ($\sim$200 K), the curves begin to curve upward after a few ps, indicating the onset of water translational diffusion with a diffusion rate that increases with temperature. It is worth noting that the protein hydration water displays anomalous diffusion at all temperatures (i.e., the slope of the mean-squared displacement versus time is less than the value of one, expected for Brownian motion). In Fig. 5b, the corresponding data for glycerol depict a similar picture, with the onset of solvent translational diffusion occurring in the vicinity of the protein dynamical transition temperature ($\sim$280 K) in glycerol.

In summary, we have used MD simulations to investigate the dependence of the dynamics of a soluble protein, RNase A, on temperature and solvent environment. Consistent with neutron scattering data, the simulations predict that the protein undergoes a dynamical transition in both glycerol and aqueous solutions that is absent in the dry protein. The temperature of the transition is higher, while the rate of increase with temperature of the amplitudes of motion on the 100 ps timescale is lower, in glycerol versus water. Analysis of the dynamics of hydrogen bonds revealed that the protein dynamical transition is connected to the relaxation of the protein–solvent hydrogen bond network, which, in turn, is associated with solvent translational diffusion. Thus, it appears that the role of solvent dynamics in affecting the protein dynamical transition is qualitatively similar in water and glycerol.

Acknowledgments This work was supported by grants CHE–0417158 and CHE-0750175 from the National Science Foundation.

References

Allen MP, Tildesley DJ (1989) Computer simulation of liquids. Clarendon, Oxford

Andersen HC (1983) Rattle: a velocity version of the shake algorithm for molecular dynamics calculations. J Comp Phys 52:24–34

Beé M (1988) Quasielastic neutron scattering: principles and applications in solid state chemistry, biology, and materials science. Adam Hilger, Bristol

Caliskan G, Kisliuk A, Sokolov AP (2002) Dynamic transition in lysozyme: role of a solvent. J Non-Cryst Solids 307:868–873

Caliskan G, Mechtani D, Roh JH, Kisliuk A, Sokolov AP, Azzam S, Cicerone MT, Lin-Gibson S, Peral I (2004) Protein and solvent dynamics: how strongly are they coupled? J Chem Phys 121:1978–1783

Chen S-H, Liu L, Fratini E, Baglioni P, Faraone A, Mamontov E (2006) Observation of fragile-to-strong dynamic crossover in protein hydration water. Proc Natl Acad Sci USA 103:9012–9016

Cornicchi E, Marconi M, Onori G, Paciaroni A (2006) Controlling the protein dynamical transition with sugar-based bioprotectant matrices: a neutron scattering study. Biophys J 91:289–297

Curtis JE, Dirama TE, Carri GA, Tobias DJ (2006) Inertial suppression of protein dynamics in a binary glycerol-trehalose glass. J Phys Chem B 110:22953–22956

Daniel RM, Dunn RV, Finney JL, Smith JC (2003) The role of dynamics in enzyme activity. Ann Rev Biophys Biomol Struct 32:69–92

Dioumaev AK, Lanyi JK (2007) Bacteriorhodopsin photocycle at cryogenic temperatures reveals distributed barriers of conformational substates. Proc Natl Acad Sci USA 104:9621–9626

Dirama TE, Carri GA, Sokolov AP (2005) Coupling between lysozyme and glycerol dynamics: microscopic insights from molecular dynamics simulations. J Chem Phys 122(24):244910

Doster W, Cusack S, Petry W (1989) Dynamical transition of myoglobin revealed by inelastic neutron scattering. Nature 337:754–756

Doster W, Cusack S, Petry W (1990) Dynamical instability of liquidlike motions in a globular protein observed by inelastic neutron scattering. Phys Rev Lett 65:1080–1083

Doster W, Settles M (1999) The dynamical transition in proteins: the role of hydrogen bonds. In: Bellissent-Funel M-C (ed) Hydration processes in biology: experimental and theoretical approaches, vol 305. IOS, Amsterdam, pp 177–191

Doster W, Settles M (2005) Protein–water displacement distributions. Biochim Biophys Acta 1749:173–186

Essmann U, Perera L, Berkowitz ML, Darden T, Pedersen LG (1995) A smooth particle mesh Ewald method. J Chem Phys 103:8577–8593

Fenimore PW, Frauenfelder H, McMahon B, Parak FG (2002) Slaving: solvent fluctuations dominate protein dynamics and function. Proc Natl Acad Sci USA 99:16047–16051

Fenimore PW, Frauenfelder H, McMahon B, Young RD (2004a) Bulk-solvent and hydration-shell fluctuations, similar to alpha- and beta-fluctuations in glasses, control protein motions and functions. Proc Natl Acad Sci USA 101:14408–14413

Fenimore PW, Frauenfelder H, McMahon BH, Young RD (2004b) Proteins are paradigms of stochastic complexity. Physica A 351:1–13

Finkelstein IJ, Massari AM, Fayer MD (2007) Viscosity-dependent protein dynamics. Biophys J 92:3652–3662

Frauenfelder H, Petsko GA, Tsernoglou D (1979) Temperature-dependent X-ray diffraction as a probe of protein structural dynamics. Nature 280:558–563

Frauenfelder H, Sligar SG, Wolynes PG (1991) The energy landscapes and motions of proteins. Science 254:1598–1603

Frauenfelder H, Fenimore PW, McMahon BH (2002) Hydration, slaving and protein function. Biophys Chem 98:35–48

Heberle J, Fitter J, Sass HJ, Büldt G (2000) Bacteriorhodopsin: the functional details of a molecular machine are being resolved. Biophys Chem 85:229–248

Knapp EE, Fischer SF, Parak F (1982) Protein dynamics from Mössbauer spectra: the temperature dependence. J Phys Chem 86:5042–5047

Kumar P, Yan Z, Xu L, Mazza MG, Buldryev SV, Chen S-H, Sastry S, Stanley HE (2006) Glass transition in biomolecules and the liquid–liquid critical point of water. Phys Rev Lett: 97(17):177802

Kurkal V, Daniel RM, Finney JL, Tehei M, Dunn RV, Smith JC (2005) Low frequency enzyme dynamics as a function of temperature and hydration: a neutron scattering study. Chem Phys 317:267–273

Lechner RE, Fitter J, Dencher NA, Hauss T (2006) Low-energy dynamics and biological function. Physica B 385–386:835–837

Lee AL, Wand AJ (2001) Microscopic origins of entropy, heat capacity and the glass transition in proteins. Nature 411:501–504

Luzar A, Chandler D (1996a) Effect of environment on hydrogen bond dynamics in liquid water. Phys Rev Lett 76:928–931

Luzar A, Chandler D (1996b) Hydrogen bond kinetics in liquid water. Nature 379:55–57

MacKerell Jr AD, Bashford D, Bellott M, Dunbrack Jr RL, Evanseck J, Field MJ, Fischer S, Gao J, Guo H, Ha S, Joseph-McCarthy D, Kuchnir L, Kuczera K, Lau FTK, Mattos C, Michnick S, Ngo T, Nguyen DT, Prodhom B, Reiher III WE, Roux B, Schlenkrich M, Smith JC, Stote R, Straub J, Watanabe M, Wiorkiewicz-Kuczera J, Yin D, Karplus M (1998) All-atom empirical potential for molecular modeling and dynamics studies of proteins. J Phys Chem B 102:3586–3616

Martyna GJ, Tuckerman ME, Klein ML (1992) Nosé-Hoover chains: the canonical ensemble via continuous dynamics. J Chem Phys 97:2635–2643

Martyna GJ, Tobias DJ, Klein ML (1994) Constant pressure molecular dynamics simulations. J Chem Phys 101:4177–4189

Martyna GJ, Tuckerman ME, Tobias DJ, Klein ML (1996) Explicit reversible integrators for extended systems dynamics. Mol Phys 87:1117–1157

Paciaroni A, Cinelli S, Onori G (2002) Effect of the environment on the protein dynamical transition: a neutron scattering study. Biophys J 83:1157–1164

Parak F (2003) Physical aspects of protein dynamics. Rep Prog Phys 66:103–129

Rasmussen BF, Stock AM, Ringe D, Petsko GA (1992) Crystalline ribonuclease A loses function below the dynamical transition at 220 K. Nature 357:423–424

Russo D, Hura GL, Copley JRD (2007) Effects of hydration water on protein methyl group dynamics in solution. Phys Rev E 75:040902

Ryckaert J-P, Ciccotti G, Berendsen HJC (1977) Numerical integration of the cartesian equations of motion of a system with constraints: molecular dynamics of *n*-alkanes. J Comp Phys 23:327–341

Smith J, Kuczera K, Karplus M (1990) Dynamics of myoglobin: comparison of simulation results with neutron scattering spectra. Proc Natl Acad Sci USA 90:9135–9139

Swenson J, Jansson H, Bergman R (2006) Relaxation processes in supercooled confined water and implications for protein dynamics. Phys Rev Lett 96:247802

Tarek M, Tobias DJ (1999) Environmental dependence of the dynamics of protein hydration water. J Am Chem Soc 121:9740–9741

Tarek M, Tobias DJ (2000) The dynamics of protein hydration water: a quantitative comparison of molecular dynamics simulations and incoherent neutron scattering experiments. Biophys J 79:3244–3257

Tarek M, Martyna GJ, Tobias DJ (2000) Amplitudes and frequencies of protein dynamics: an analysis of discrepancies between neutron scattering and molecular dynamics simulations. J Am Chem Soc 102:10450–10451

Tarek M, Tobias DJ (2002) Role of protein–water hydrogen bond dynamics in the protein dynamical transition. Phys Rev Lett 88:138101

Tournier AL, Xu J, Smith JC (2003) Translational water dynamics drives the protein glass transition. Biophys J 85:1871–1875

Tsai AM, Neumann DA, Bell LN (2000) Molecular dynamics of solid-state lysozyme as affected by glycerol and water: a neutron scattering study. Biophys J 79:2728–2732

Tuckerman ME, Yarne DA, Samuelson SO, Hughes AL, Martyna GJ (2000) Exploiting multiple levels of parallelism in molecular dynamics based calculations via modern techniques and software paradigms. Comp Phys Comm 128:333

Wlodawer A, Svensson LA, Sjolin L, Gilliland G (1988) Structure of phosphate free ribonuclease A refined at 1.26 Å resolution. Biochemistry 27:2705–2717

Wood K, Frölich A, Paciaroni A, Moulin M, Härtlein M, Zaccaï G, Tobias DJ, Weik M (2008) Coincidence of dynamical transitions in a soluble protein and its hydration-water: direct measurements by neutron scattering and MD simulations. J Am Chem Soc 130:4586–4587

Wuttke J, Petry W, Coddens G, Fujara F (1995) Fast dynamics of glass-forming glycerol. Phys Rev E 52:4026–4034

Zanotti J-M, Bellissent-Funel MC, Chen SH (2005) Experimental evidence of a liquid–liquid transition in interfacial water. Europhys Lett 71:91–97